

Generation of Magnetic Noise Bursts During Distant Rocket Launches

Pilipenko, V.⁽¹⁾, Fedorov, E.⁽¹⁾, Mursula, K.⁽²⁾, and Pikkarainen, T.⁽²⁾

¹Institute of the Physics of the Earth, Moscow, Russia

²University of Oulu, Finland

(Received: June 2005; Accepted: November 2005)

Abstract

Bursts of hydromagnetic noises in the frequency range around 1 Hz after distant rocket launches have been detected at remote ground-based observatories. Theoretical model is suggested which interprets this phenomenon as generation of fast compressional waves by expanding waste products injected by rocket boosters into the ionosphere and their subsequent trapping into the ionospheric magnetosonic waveguide.

Key words: modification of the ionosphere, Pc1 pulsations, rocket-induced disturbances, ionospheric MHD waveguide

1. Introduction

Any intense impact on the ionosphere, e.g. acoustic blast waves from natural or artificial sources (*Pokhotelov et al.*, 1994), is accompanied by occurrence of electromagnetic disturbances. Injection of ionizing (Ba, Li, Na,...) or plasma suppressive (H_2O , ...) compounds also results in a whole complex of phenomena: generation of MHD impulse (*Kelley et al.*, 1980), burst of ELF electromagnetic noise (*Koons and Pongratz*, 1979), plasma turbulization, and stimulation of energetic particle precipitation (*Yau et al.*, 1988; *Danilushkin et al.*, 1988; *Kozlov and Smirnova*, 1992).

Powerful source of the ionosphere modification is rocket launches. The mechanisms of the rocket-induced distortions of the ionosphere (*Yau et al.*, 1981) and terrestrial electromagnetic field (*Dea et al.*, 1991) studied so far were related to acoustic disturbances from fast flying rocket or enhanced plasma recombination due to waste products (*Mendillo*, 1988; *Karlov et al.*, 1980; *Blagoveschenskaya et al.*, 1990; *Gorelyi et al.*, 1994).

Take-offs of powerful rockets are accompanied by a throw into the upper atmosphere of clouds comprising exhaust gases and dust. These clouds result in the occurrence of unusual optical phenomena owing to their interaction with the upper atmos-

phere and sunlight scattering. These optical phenomena were often noticed at different altitudes during polar aurora observations in northern parts of the Soviet Union after rocket launches from Plesetsk site (*Vetchinkin et al.*, 1993; *Tagirov et al.*, 2000). Bright optical phenomena (often seen from distances up to 10^3 km) used to be detected at altitudes 100-120 km in twilight. According to optical observations the expansion velocity of the waste product cloud was ~ 1 -2 km/s and its typical scale reached ~ 100 -200 km. The switch-off of rocket boosters at altitudes > 150 km resulted in an instantaneous throw into the ionosphere of large amount (hundreds of kg) of the waste products (*Smirnova et al.*, 1995). The resulting waste clouds expanded with velocity 2-3 km/s, and could reach altitudes up to ~ 700 km with transverse scales ~ 1500 km (*Mendillo et al.*, 1975).

In this paper we draw attention to another possible effect of an active impact on the ionosphere from rocket launch - excitation of magnetosonic waveguide in the ionosphere, which transmits electromagnetic disturbances in the Hz frequency band to considerable distances.

2. *Bursts of magnetic noises during rocket launches*

For the study of the possibility of geomagnetic pulsations generation we made a retrospective analysis of the mid-latitude geomagnetic observatories data according to the list of powerful strategic missile launches from the rocket site Plesetzsk (180 km southward from Arkhangelsk, Northern Russia) from February 1989 to February 1991. We analyzed the data of magnetic observatories Sodankila (SOD, geographic coordinates $67.37^\circ, 26.63^\circ$) and Oulu (OUL, $64.52^\circ, 27.23^\circ$), situated about 10^3 km to west-south from launching site. At these observatories the high frequency ULF pulsations are recorded with the use of search-coil magnetometers with sensitivity ~ 1 pT. The paper-chart recording is performed with speed 24 inch/hour (basic) and 6 inch/hour (additional). The signals are recorded on analogue magnetic tape which gives possibility to perform with an analogue electronic sonograph analyzer a spectral analysis of selected events in the frequency range from 0.01 Hz to 1.5 Hz. Ambiguity of the signal onset determination during sonographic analysis is about 1 min.

Within the frequency band under study the natural emissions (Pi1C, Pi1B, Pc1, and IPDP pulsations) are often observed (*Bosinger et al.*, 1981). Therefore we excluded from the consideration the events during substorm activity at higher latitudes in a given sector of the magnetosphere. In a few events remained the occurrence of weak signals in Hz frequency range after rocket launches were noticed. Keeping in mind the uncertainty of take-off moments about few minutes, we suppose that an onset of probable stimulated emission should be within 10 min interval after a nominal take-off.

Fig. 1 shows the H component magnetogram and sonogram from observatory SOD during the launch (1930 UT) on November 01, 1989. About 10 min after the nominal take-off (which is marked by triangle) a short-lived isolated burst of emission with ~ 5 min duration is observed. The signal is detected on a quite background. Only

about 2 hours later, at 2120 UT a series of regular P1c emission begins. At more distant observatory OUL no signal could be reliably retrieved in this time interval.

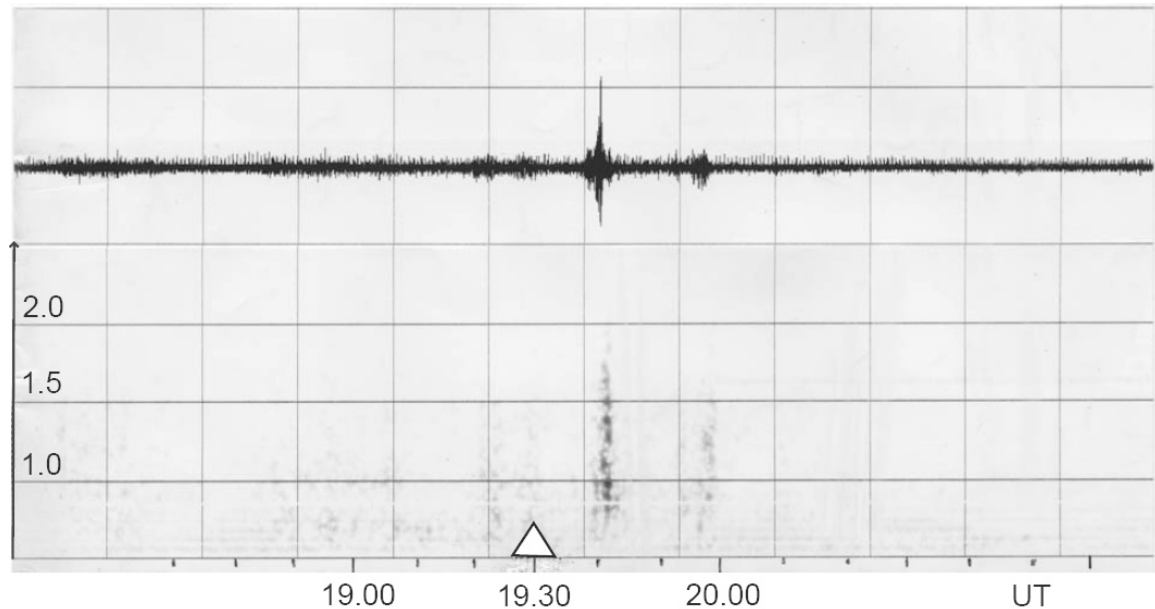


Fig. 1. Magnetic noise signal detected at SOD observatory during the rocket launch on November 01, 1989: (upper plot) H component magnetogram 1800-2200 UT, and (bottom plot) corresponding sonogram in the frequency range from 0.01 Hz to 1.5 Hz. The take-off moment (1930 UT) is marked by a triangle.

Similar effects were revealed during several other launches as well. Commonly, the anomalous emission was rather weak and could be isolated from the background only with the help of sonographic analysis. Further we discuss the principal physical possibility of the generation of geomagnetic noises by a running rocket engine in the ionosphere.

3. *Modification of the ionospheric plasma and excitation of MHD modes*

The movement of rocket with running engine through the ionosphere can be visualized as a continuous sequence of neutral gas injections along the trajectory. The effectiveness of the hydromagnetic disturbances excitation at different stages of the fly apart of rocket engine waste depends on the dynamics of the movement of the neutral gas component introduced into the ionosphere. At first stage, the expanding gas "grabs" the ionospheric plasma as a "snow plow", and then hampers gradually. When the energy of the expelled plasma becomes comparable with the energy of injection, the gas expansion stops and then the diffusion of this gas into the ionospheric plasma takes place. The injected neutral component involves into movement both the electron and ion constituents of the background plasma. For the consideration of the neutral cloud expansion in the ionosphere a reverse influence of an ionized component on the dynamics of neutrals can be neglected.

For the description of the neutral component dynamics it can be supposed for simplicity that expanding gas is a cylindrical cloud with time-varying radius $R_m(t)$. The known solution of the acoustical problem about fly apart of neutral gas enables one to consider the time variations of the frozen-in parameters for electrons v_{em}/Ω_e and ions v_{in}/Ω_i , where Ω_i and Ω_e are gyrofrequencies of ions and electrons, and v_{en} , v_{in} are collision frequencies with neutrals.

The time variations of the frozen-in parameters naturally retrieve three stages in the evolution of the ionized component dynamics:

- (1) $0 < t < \tau_1$ - both ions and electrons are non-magnetized;
- (2) $\tau_1 < t < \tau_2$ -magnetized electrons and non-magnetized ions;
- (3) $t > \tau_2$ -both electrons and ions are frozen into the magnetic field.

Because τ_1 is very small, one may consider that just after the injection electrons remain magnetized and ions are non-magnetized up to the moment $\tau_2 \sim 0.5$ s. Only at this stage an electric current is generated.

Formation of "plasma hole"

The dynamics of ionospheric ionized components can be described with the use of three-fluid hydrodynamics of cold collisional plasma, consisting from electrons, ions and neutrals. The velocity of neutrals V_n is assumed to be determined by non-plasma processes. Disturbed concentrations of electrons n_e and ions n_i are related to their fluxes by the continuity equations

$$\frac{\partial n_e}{\partial t} + \nabla \mathbf{U}_e = q, \quad \frac{\partial n_i}{\partial t} + \nabla \mathbf{U}_i = q \quad (1)$$

where q stands for the rate of ionization/recombination processes. The particle flows are

$$\mathbf{U}_e = n_e \mathbf{V}_{e0} - \hat{\sigma}_e \mathbf{E}_c / e, \quad \mathbf{U}_i = n_i \mathbf{V}_{i0} + \hat{\sigma}_i \mathbf{E}_c / e \quad (2)$$

Here the bulk electron and ion velocities, produced by movement of neutrals and background ionospheric electric field \mathbf{E}_0 , can be determined via the tensors of electron and ion conductivity, $\hat{\sigma}_e$ and $\hat{\sigma}_i$, as follows:

$$\mathbf{V}_{e0} = \mathbf{V}_n - \frac{\hat{\sigma}_e}{en_e} (\mathbf{E}_0 + \mathbf{V}_n \times \mathbf{B}_0), \quad \mathbf{V}_{i0} = \mathbf{V}_n + \frac{\hat{\sigma}_i}{en_i} (\mathbf{E}_0 + \mathbf{V}_n \times \mathbf{B}_0) \quad (3)$$

The polarization electric field \mathbf{E}_c , arising due to the plasma inhomogeneity, can be determined from the Poisson's equation $\nabla \cdot \mathbf{E}_c = -e(n_e - n_i)$. We have neglected a slow diffusion process caused by density or temperature gradients.

The above equations (1-3) together with Maxwell's equations enable one to describe the dynamics of plasma and electromagnetic field in the region of neutral gas injection into the ionosphere. However, in a general situation the solutions can be

obtained only with numerical methods, so we will try to outline possible ways to construct an approximate analytical theory.

Thanks to the plasma quasi-neutrality, $n \simeq n_e \simeq n_i$, this system can be simplified, and instead of two equations (1) one gets

$$\frac{\partial n}{\partial t} + \nabla \cdot \mathbf{U} = 0 \quad (4)$$

The equation for the electric field potential $\mathbf{E}_c = -\nabla\Phi_c$ can be obtained with account for (2-4) as follows

$$\nabla \cdot (\hat{\sigma} \nabla \Phi_c) = \nabla \cdot [\hat{\sigma} \{ \mathbf{E}_0 + \mathbf{V}_n \times \mathbf{B}_0 \}] \quad (5)$$

where $\hat{\sigma} = \hat{\sigma}_e + \hat{\sigma}_i$. Combining the above relationships (4-5) we obtain

$$\frac{\partial n}{\partial t} + \nabla \cdot \left\{ n \left[\mathbf{V}_n + \frac{\hat{\sigma}_i - \hat{\sigma}_e}{2ne} (\mathbf{E}_0 + \mathbf{V}_n \times \mathbf{B}_0) \right] \right\} = q \quad (6)$$

The equation (6) describes three stages of plasma dynamics. At first stage, when the density of neutrals is high, the collision frequencies are large, that is $\nu_{en} \gg \Omega_e$, and $\nu_{in} \gg \Omega_i$. Plasma particles are dragged by neutral component and the flux caused by dynamo-field is small as compared with the one caused by \mathbf{V}_n . In this case the equation (6) reduces to the following

$$\frac{\partial n}{\partial t} + \nabla \cdot n \mathbf{V}_n = 0$$

In the case when plasma is completely dragged by a movement of neutrals, the front of an expanding neutral cloud acts as "snow plow" on a background ionospheric plasma. Near the front a closed Pedersen current is generated, which decreases the magnetic field inside the cloud, forming a "magnetic cavern", and increases it outside.

At the second stage, when $\nu_{en} < \Omega_e$ and $\nu_{in} > \Omega_i$, the electrons become magnetized, but the ions are still dragged by neutrals. Due to a charge separation an electric field E_c arise. This dynamo-field and the electron Hall conductivity produce a radial current and variation of plasma density.

At the third stage, both electron and ions become magnetized, while neutral component is still expanding. The Pedersen conductivity is low, whereas the electron and ion Hall conductivities are equal and have opposite signs. Hence, as follows from (6), the plasma concentration does not change noticeably, i.e. $\partial n / \partial t \rightarrow 0$. At this stage a neutral gas interacts with plasma weakly, so diffusion and recombination processes become important.

4. Intensity of hydromagnetic emission induced by the waste products injection

Principal feature of the ionosphere for the propagation of MHD waves is the non-monotonic dependence of Alfvén velocity V_A on altitude: it increases from a few of 10^2 km/s at $z \geq 150$ km to a few of 10^3 km/s at $z \simeq 10^3$ km. The non-monotonic variation of $V_A(z)$ ensures the occurrence of the waveguide and resonator for MHD waves in the F-layer of the ionosphere. At a steep gradient of $V_A(z)$ at height z_A , where the geometric optic approximation is violated, Alfvén wave partially reflects back, thus forming the ionospheric Alfvén resonator (IAR) at frequencies $f^{(A)} \simeq V_A/(z_A - h) \sim 1$ Hz (that is Pc1 frequency range of geomagnetic pulsations), where h is the height of the conductive layer of the ionosphere (*Belyaev et al.*, 1999).

At the same time, fast magnetosonic waves can undergo total reflection at some height, and be trapped in the ionospheric waveguide in the F-layer. The critical cut-off frequency of the wave guide $f^{(M)}$ is related to the eigenfrequency of the IAR as follows $f^{(A)} \simeq f^{(M)} \cos I$, where I is the inclination of geomagnetic field. The early experiments showed that Pc1 waves trapped into the F-layer waveguide can propagate with a low attenuation to distances up to a few of 10^3 km (*Greinfinger and Greinfinger*, 1968).

Now we consider a principal possibility of the magnetosonic waveguide excitation and outline the theoretical approach for an analytical description of this process. In a qualitative way the movement of rocket can be visualized as a continuous sequence of micro-injections of neutral gas from rocket engine and an accompanying excitation of short-lived ($\sim \tau_2$) bursts of electric currents. At later times the engine waste fly apart transfers into a diffusive spreading, and the plasma density decreases due to enhanced recombination with the waste products, producing the "water hole" (*Mendillo*, 1975). This later stage will not be considered here.

The first stage of a fly-apart can be described by the snow-plow model. The movement of a plasma plow excites electric fields and currents which generate hydromagnetic emission from an injection region. The density of excited currents are determined by

$$\mathbf{J}_0 = \sigma[\mathbf{E}_0 + \mathbf{V}_n \times \mathbf{B}_0] \quad (8)$$

The expanding cylindrical shell elongated along a rocket trajectory generates the system of radial Hall currents and azimuthal Pedersen currents (*Borisov et al.*, 1988), as illustrated in Fig. 2. The radial Hall current generates disturbances of Alfvén type (A), leaking along field lines into the magnetosphere. This type of disturbances can be responsible for an excitation of the IAR, stimulation of electrostatic turbulence, and precipitation of energetic particles. These disturbances are spatially localized and cannot be detected at distant stations.

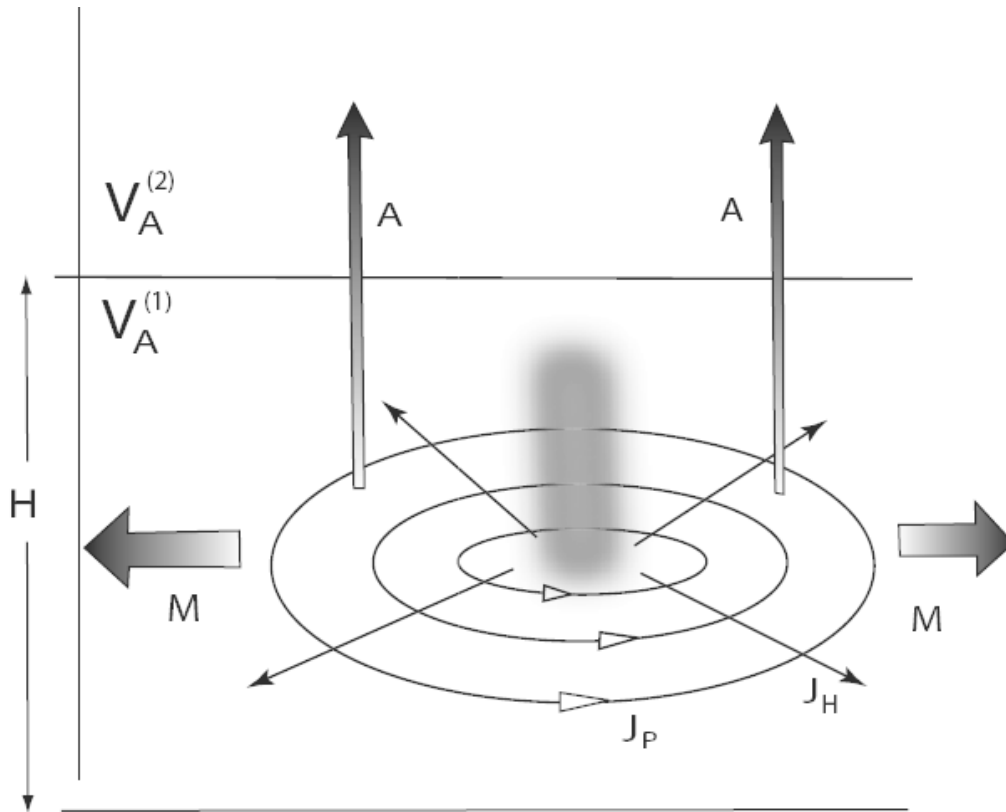


Fig. 2. A sketch of ionospheric currents generated by a radial expansion of a cylindrical rocket waste column. The radial Hall currents produce Alfvén type disturbances, and vortex Pedersen current produce magnetosonic type disturbances.

The system of the azimuthal Pedersen currents forms an effective magnetic dipole, generating magnetosonic disturbances (M). These magnetosonic waves can be trapped into the magnetosonic waveguide in the upper ionosphere and propagate along it to considerable distances.

The sequence of short-lived impulses of electric currents, generated at the initial stage of waste products fly-apart in the conductive ionosphere, results in the excitation of wide-band electromagnetic disturbances in the frequency range $f < \tau_2^{-1} \sim 2$ Hz. Then, part of these disturbances can be trapped into the ionospheric magnetosonic waveguide. As a result, one may expect to observe the signals with frequencies above the critical waveguide frequency $f > f^{(M)} \sim 0.5$ Hz at large distances from a point of rocket entry into the conductive ionosphere.

Quantitative description of the generation and transformation of electromagnetic fields by a moving source in the inhomogeneous ionosphere is a rather complicated problem, which can be treated only numerically. Below, we outline a simplified approach to this problem, which enables one to obtain analytical estimates. This estimate indicates a principal possibility of the ionospheric waveguide excitation in the Pc1 frequency band by rocket launches.

For the analytical consideration of the magnetosonic waveguide excitation by non-steady currents, produced by neutral gas injection into the ionosphere, we consider the following model (Fig. 2). The axis z of the Cartesian coordinate system is oriented along the vertical homogeneous geomagnetic field, $\mathbf{B}_0 = B_0 \mathbf{e}_z$. The ionosphere is assumed to be a horizontally stratified medium, that is V_A and $\hat{\sigma}$ depend on altitude z only. For this system the Maxwell's equation are as follows

$$(\nabla \times \mathbf{B})_{\perp} = V_A^{-2} \partial_t \mathbf{E}_{\perp} + \mu_0 \hat{\sigma}_{\perp} \mathbf{E}_{\perp} + \mu_0 \mathbf{j}^{(d)}, \quad \nabla \times \mathbf{E}_{\perp} = \partial_t \mathbf{B} \quad (9)$$

where $\hat{\sigma}_{\perp} \mathbf{E}_{\perp} = \sigma_P \mathbf{E}_{\perp} + \sigma_H [\mathbf{e}_z \times \mathbf{E}_{\perp}]$. The external current $\mathbf{j}^{(d)}$, induced by the gas expansion is assumed to be azimuthally symmetric, and can be naturally described in a local cylindrical coordinate system $\{r, \varphi, z\}$ with axis z along the symmetry axis.

For the description of electric and magnetic fields of MHD waves we introduce the scalar Φ and vector \mathbf{A} potentials: $\mathbf{B} = \nabla \times \mathbf{A}$, and $\mathbf{E} = -\nabla \Phi - \partial_t \mathbf{A}$. In fact, the scalar potential Φ and vertical component of the vector potential $\mathbf{A}_z = A \hat{\mathbf{e}}_z$ are potentials of a shear Alfvén mode, whereas the perpendicular component of \mathbf{A}_{\perp} is the potential of a magnetosonic (compressional) mode. For the gauge calibration condition $\nabla \cdot \mathbf{A}_{\perp} = 0$, the component \mathbf{A}_{\perp} can be expressed through the magnetosonic scalar potential Ψ as follows $\mathbf{A}_{\perp} = \hat{\mathbf{z}} \times \nabla \Psi$. The total wave electromagnetic fields can be presented as a sum of Alfvén and magnetosonic modes

$$\begin{aligned} \mathbf{E}_{\perp} &= -\nabla_{\perp} \Phi + \hat{\mathbf{e}}_z \times \nabla_{\perp} \partial_t \Psi \\ \mathbf{B} &= -\hat{\mathbf{e}}_z \times \nabla_{\perp} A + \nabla_{\perp} \partial_z \Psi - \hat{\mathbf{z}} \nabla_{\perp}^2 \Psi \\ E_z &= -\partial_z \Phi - \hat{\mathbf{e}}_z \partial_t A \end{aligned} \quad (10)$$

We assume that the external current $\mathbf{j}^{(d)}$ is divergence-free, that is $\nabla_{\perp} \cdot \mathbf{j}^{(d)} = 0$, therefore a potential $U^{(d)}$ for this current can be introduced as follows $\mathbf{j}^{(d)} = \hat{\mathbf{e}}_z \times \nabla_{\perp} U^{(d)}$. Substituting (10) into (9) and applying to the obtained equations the operators $(\nabla_{\perp} \cdot \dots)$ and $[\nabla_{\perp} \times \dots]$, we get the system of coupled equations for potentials

$$\begin{aligned} \partial_z A + V_A^{-2} \partial_t \Phi + \mu_0 \sigma_P \Phi + \mu_0 \text{sign}(B_{0z}) \sigma_H \partial_t \Psi &= 0 \\ \nabla_{\perp}^2 \Psi - V_A^{-2} \partial_t^2 \Psi - \mu_0 \sigma_P \partial_t \Psi - \mu_0 \text{sign}(B_{0z}) \sigma_H \Phi &= \mu_0 U^{(d)} \\ \partial_t A + \partial_z \Phi &= 0 \end{aligned} \quad (11)$$

Differentiating of (11) by time we get

$$\begin{aligned} \partial_z^2 \Phi - V_A^{-2} \partial_t^2 \Phi - \mu_0 \sigma_P \partial_t \Phi - \mu_0 \text{sign}(B_{0z}) \sigma_H \partial_t^2 \Psi &= 0 \\ \nabla_{\perp}^2 \Psi - V_A^{-2} \partial_t^2 \Psi - \mu_0 \sigma_P \partial_t \Psi - \mu_0 \text{sign}(B_{0z}) \sigma_H \Phi &= \mu_0 U^{(d)} \end{aligned} \quad (12)$$

This system of equations shows that two MHD modes are coupled in the ionosphere owing to the Hall conductivity $\sigma_H \neq 0$.

The boundary conditions for the potentials that must be satisfied at the interface $z = -l_i$ between the atmosphere and ionosphere are deduced from the equations describing E and B fields in the Earth and atmosphere. The first boundary condition at the bottom edge of the ionosphere denotes the current non-penetration into the atmosphere, $j_z(z = -l_i) = 0$. Using the relationship $\mu_0 \mathbf{j}_z = -\nabla_{\perp}^2 A$, this boundary condition can be re-formulated as $A(z = -l_i) = 0$. The use of this condition and (10) yields $\partial_z \Phi(z = -l_i) = 0$.

The second boundary condition is more complex and follows from the impedance matching. We assume that the condition $\partial_z \Psi/\Psi = \nu \cot(\nu h)$ is satisfied $z = -l_i$, where ν is the horizontal wave vector. When $\nu h \ll 1$, the latter boundary condition reduces to $\partial_z \Psi/\Psi = 1/h$.

Let us suppose that the external current potential $U^{(d)}$ has the form as $U^{(d)} = -M(t)(2\pi r_0)^{-1} \delta(\mathbf{r} - \mathbf{r}_0)$, where $M(t)$ is its magnetic moment located at $z = z_0$, $r = r_0$. For the chosen potential the induced current has the azimuthal component only, namely $j_{\varphi}^{(d)} = \partial r U(r)$. The effective magnetic moment of this current is

$$M\mathbf{e}_z = \frac{1}{2} \int [\mathbf{r} \times \mathbf{j}^{(d)}(r)] dV = -2\pi \mathbf{e}_z \iint U(r) r dr dz \quad (13)$$

For the study of hydromagnetic wave generation in the ionospheric waveguide we consider the excitation of waveguide magnetosonic modes, neglecting their coupling with Alfvén disturbances due to the Hall conductivity. Thus, in (12) we omit the term $\propto u_0 \sigma_H \Phi$. Then the magnetosonic potential Ψ can be found from the following boundary problem

$$\begin{aligned} \nabla^2 \Psi - V_A^{-2} \partial_z^2 \Psi &= -\mu_0 M(t) \delta(\mathbf{r} - \mathbf{r}_0) \\ \Psi(z=0) &= \alpha \partial_z \Psi \end{aligned} \quad (14)$$

where $\alpha = (1/h - i\omega\mu_0\Sigma_p)^{-1}$ for $\nu h < 1$. For a dayside highly-conductive ionosphere $|\omega\mu_0\Sigma_p| \gg 1/h$, whereas for a nightside low-conductive ionosphere an opposite inequality holds. After Fourier transform over time, we obtain in cylindrical coordinates

$$\begin{aligned} \frac{1}{2} \partial_r (r \partial_r \Psi) + \partial_z^2 \Psi + k_A^2 \Psi &= -\mu_0 (2\pi r_0)^{-1} M(\omega) \delta(z - z_0) \\ \Psi(z=0) &= \alpha \partial_z \Psi \end{aligned} \quad (15)$$

The potential Ψ can be searched as sum of waveguide modes, determined by the boundary Sturm-Liouville problem

$$\partial_z^2 u + k_A^2 u = v^2 u, \quad u(z=0) = \alpha \partial_z u \quad (16)$$

The eigenvalues v_n^2 (wave vectors of n -th mode) correspond to orthogonal eigenfunctions $u_n(z)$. The spectrum of this mathematical problem consists of continuous and discrete (waveguide modes) parts, so the potential Ψ can be presented as a sum of normal modes

$$\Psi = \sum a_n(r) U_n(z) + \int \{\text{over continuous spectrum}\} \quad (17)$$

Substituting of the Ψ decomposition (17) into (16), then multiplying the obtained relationship by $u_n(z)$, integrating it over z , and using the orthogonality condition, we obtain the following

$$r^{-1} \partial_r (r \partial_r a_n) + v_n^2 a_n = \mu_0 M(\omega) (2\pi r_0)^{-1} \delta(r - r_0) u_n(z_0) \quad (18)$$

where $u_n(z_0)$ is the magnitude of the waveguide eigenmode at the altitude of a source. The solution of (18) can be expressed through the Green's function of the Bessel's equation $G(r, r_1)$ as follows

$$a_n(r) = -\mu_0 M(\omega) (2\pi r_0)^{-1} u_n(z_0) \int_0^\infty G(r, r_1) \delta(r_1 - r_0) r_1 dr_1 \quad (19)$$

where

$$G(r, r_1) = \frac{\pi}{2i} \begin{cases} H_0^{(1)}(v_n r) J_0(v_n r_1) & \text{at } r_1 > r \\ H_0^{(1)}(v_n r_1) J_0(v_n r) & \text{at } r > r_1 \end{cases}$$

At $r > r_1$, i.e. outside the region occupied by the current $\mathbf{j}^{(d)}$, from (19) one can obtain the coefficient of the n -th mode excitation

$$a_n(r) = i \frac{\mu_0}{4} M(\omega) u_n(z_0) H_0(v_n r) \quad (20)$$

The potential of the n -th waveguide mode can be finally obtained after substitution of the latter expression (20) into (17)

$$\Psi_n(r, z) = i \frac{\mu_0}{4} M(\omega) u_n(z_0) u_n(z) H_0(v_n r) \quad (21)$$

At $v_n r \gg 1$, i.e. in the far-field zone, the Hankel's function can be replaced by its asymptotic decomposition for large argument as follows

$$\Psi_n(r, z) \simeq \frac{\mu_0}{4} M(\omega) u_n(z_0) u_n(z) \sqrt{\frac{2}{\pi v_n r}} \exp(i v_n r + i \frac{\pi}{4}) \quad (22)$$

For an arbitrary vertical profile of $V_A(z)$ the effectiveness of the waveguide excitation can be estimated only with the numerical calculations. Therefore, we derive the analytical expressions for the waveguide excitation coefficient for the simplified two-layer ionospheric model.

5. Two-layer model of the ionosphere

Let the vertical profile of $V_A(z)$ in a step-wise waveguide is as follows

$$V_A(z) = \begin{cases} V_1 & \text{at } 0 > z > H \\ V_2 & \text{at } H > z > \infty \end{cases} \quad (23)$$

Then, the vertical structure of the waveguide mode potential has the following form

$$u_n(z) = N_n^{-1} \begin{cases} \cos[\kappa_n(z-H)] - \frac{q_n}{\kappa_n} \sin[\kappa_n(z-H)] & \text{at } 0 > z > H \\ \exp[-q_n(z-H)] & \text{at } H > z > \infty \end{cases} \quad (24)$$

where $\kappa(v) = \sqrt{\omega^2/V_1^2 - v^2}$, and $q(v) = \sqrt{v^2 - \omega^2/V_2^2}$ are effective inverse vertical scales in one of layers. The horizontal wavenumbers of the waveguide modes v_n lay within the range $\omega/V_2 < v_n < \omega/V_1$. The normalization factor in (24) is as follows

$$N_n^2 = \frac{H}{2} \left[1 + \frac{q_n^2}{\kappa_n^2} + \left(1 - \frac{q_n^2}{\kappa_n^2} \right) \frac{\sin 2\kappa_n H}{2\kappa_n H} + \frac{2q_n \sin^2(\kappa_n H)}{\kappa_n^2 H} \right] \quad (25)$$

Dispersion equation for the waveguide numbers v_n can be obtained by substituting $u_n(z)$ into the boundary condition

$$\frac{\kappa_n \cos \kappa_n H + q_n \sin \kappa_n H}{\kappa_n (\kappa_n \sin \kappa_n H - q_n \cos \kappa_n H)} = \alpha \quad (26)$$

The space-time distribution of the waveguide mode potential $\Psi_n(t, r, z)$ can be found with the inverse Fourier transform of (22)

$$\Psi_n(t, r, z) = \frac{\mu_0}{4\sqrt{2\pi}} \int_{-\infty}^{\infty} d\omega M(\omega) u_n(z_0) u_n(z) \sqrt{\frac{2}{\pi v_r}} \exp i(v_n r + \frac{\pi}{4} - \omega t) \quad (27)$$

The relationship obtained proves the principal possibility of the magnetosonic waveguide excitation by a firing rocket engine. The developed mathematical formalism can be used for quantitative estimate under specific parameters of the rocket engine waste products.

6. Relative efficiency of the waveguide mode excitation

To provide some idea about an efficiency of the MHD wave power trapping into the ionospheric waveguide we compare the energy of the excited waveguide mode with the total energy emitted by an effective magnetic dipole.

Let $S_n(r)$ is the time-averaged energy flux transported by the n -th waveguide mode in the F-layer through the lateral surface of a cylinder with radius r in coordinate notations

$$S_n(r) = \frac{\pi}{\mu_0} r \int_0^{\infty} E_{\varphi} B_z^* dz$$

We substitute in this relationship the field components via the potential Ψ

$$E_{\varphi} = -i\omega \partial_r \Psi_n, \quad B_r = \partial_{rz}^2 \Psi_n, \quad B_z = -\frac{1}{r} \partial_r (r \partial_r \Psi_n),$$

and obtain the energy flux across the cylinder boundary

$$S_n(r) = \text{Re} \left(i\omega \frac{\pi}{\mu_0} \int_0^{\infty} \partial_r \Psi_n \partial_r (r \partial_r \Psi_n^*) dz \right) \quad (28)$$

Substituting Ψ_n from (22) into (28) and taking into account that $\partial_r \Psi_n = i\nu_n \Psi_n$ and $\partial_r (r \partial_r \Psi_n) = -\nu_n^2 r \Psi_n$ we find

$$S_n(r) = \frac{\mu_0 \omega}{8} |\nu_n M u_n(z_0)|^2 \exp[-2\text{Im}(\nu_n)r] \quad (29)$$

We normalize the energy flux (29) by the power of a magnetic dipole emission in a space with constant Alfvén velocity V_A . The potential Ψ produced by this dipole in a homogeneous space is

$$\Psi = \mu_0 M \frac{\exp(ik_A R)}{R} \quad R = (r^2 + z^2)^{1/2}$$

Because in the far-field zone $\partial_r \Psi \simeq ik_A \Psi$, the field components may be presented as follows

$$E_{\varphi} \simeq \frac{r}{R} \frac{\omega^2}{V_A} \Psi, \quad B_r \simeq -\frac{rz}{R^2} \frac{\omega^2}{V_A^2} \Psi, \quad B_z \simeq \frac{r^2}{R^2} \frac{\omega^2}{V_A^2} \Psi.$$

Using these relationships we obtain a formula for the Poynting vector of the magnetic dipole radiation

$$\mathbf{S} = \frac{1}{2\mu_0} \operatorname{Re}(\mathbf{E} \times \mathbf{B}^*) = \frac{\omega^4}{V_A^3} \sin^2 \theta |\mu_0 M \Psi|^2 \frac{\mathbf{R}}{R}$$

where θ is the polar angle, measured from the axis z . After integration over sphere with radius R , we find the total power emitted by harmonic dipole

$$P_\omega = \frac{8\pi}{3} \mu_0 |M(\omega)|^2 \frac{\omega^4}{V_A^3} \quad (30)$$

The relative rate of the energy carried away by the n -th waveguide mode as compared with the magnetic dipole emission intensity can be found from (29) and (30) as follows

$$\frac{S_n}{P_\omega} = \frac{3\pi}{2} \frac{|v_n|^2}{k_A^3} |u_n(z_0)|^2 \quad (31)$$

The relationship (31) shows that the waveguide excitation rate depends on relative position of the rocket in respect to the waveguide eigenmode vertical structure. For the dayside ionosphere with a high E-layer conductance it can be estimated that $|u_n(z_0)|^2 = |\alpha \partial_z u_n(z_0)|^2 \simeq \kappa_1^2 (\omega^2 \mu_0^2 \Sigma_P^2 H)^{-1}$.

Now we estimate roughly the relative energy losses by a dipole for the excitation of a fundamental ($n=1$) waveguide mode. From (31) we find

$$\frac{S_n}{P_\omega} \simeq \frac{3\pi}{2} \left| \frac{v_n^2 \kappa_n}{k_1^3} \frac{\kappa_n}{\omega^2 \mu_0^2 \Sigma_P^2 H} \right| \quad (32)$$

Let us suppose that $H = 500$ km, $V_1 = 500$ km/s, $V_2 = 1500$ km/s, $\omega = 5\text{s}^{-1}$, and $\Sigma_P = 10$ S. For this set of parameters the excitation of a waveguide mode with vertical scale $\kappa_1 H \simeq 2.6$ and horizontal wave number $v_1 H \simeq 4.3$ is possible. According to (32), the estimated relative rate of the fundamental mode excitation is rather high, that is $S_1/P_\omega \simeq 0.67$. A similar estimate for the nightside ionospheric conditions, when $|\omega \mu_0 \Sigma_P \ll |h^{-1}|$, gives a somewhat higher magnitude of the waveguide emission rate. The horizontal scale of the waveguide mode, $v_1^{-1} \simeq H/4.3 \simeq 120$ km, is comparable with the height of the ionosphere. Thus, this disturbance will be only weakly geometrically attenuated upon the propagation from the ionosphere to the ground.

7. Discussion and conclusion

The physical nature of the considered process is similar to the initial stage of ionizing compound (e.g., Ba^+) fly-apart after an explosive-like injection into the ionosphere. The characteristic time of Ba photoionization is rather large, ~ 20 s, so initially injected compound also expands as a neutral cloud. The numerical modeling made by *Grebnev and Henkin* (1999), and *Zamyshlyayev et al.* (1993) showed that at

these small times at the front of the injected mixture the plasma was compressed by several orders of magnitude. This effect can be visualized as a "snow plow" according to *Kelly et al.* (1980). At the front of the expanding cloud intense currents are generated. The azimuthal vortex current causes the formation of diamagnetic cavern inside the cloud - depression of the geomagnetic field by an order of magnitude. Only at later times a plasma diffusion and particle ionization reveal themselves, which results in the smearing of electric currents at the front of the cloud.

From the wide band electromagnetic noise generated by rocket jet at ionospheric altitudes only the oscillations with the frequencies corresponding to characteristic waveguide frequencies (~ 1 Hz) would be trapped and further propagate at larger distances. We observed the intensification of ULF activity after rocket launches just in the frequency band indicated. The supposed source of the hydromagnetic noise is the firing rocket engine during the entry into the conductive ionospheric layer.

The sonogram also shows a more weak signal at 2000 UT. One should keep in mind that the actual waveguide excitation rate depends on many hardly known factors, e.g. on relative position of the rocket in respect to the eigenmode vertical structure, and therefore could be rather inhomogeneous in time. To identify reliably any detected wave burst, a detailed information on the rocket trajectory and ionospheric parameters would be necessary.

Theoretical models and observations at widely separated stations (*Greinfinger and Greinfinger*, 1968; *Fujita*, 1988) do indicate the possibility of Pc1 wave propagation at distances about several thousands of km. According to the proposed scenario the observed signals should have a cut-off frequency, which fits the observations. It should be mentioned that an alternative mechanism of the ionospheric currents modulation by acoustic waves emitted by rocket engine cannot interpret the long-range propagation of signals.

The presented observational results and theoretical estimates cannot be considered as a convincing evidence of feasibility of this effect. We hope that further studies would help to reveal it unambiguously.

Acknowledgements

This study was supported by the RFBR grant 04-05-64321. Useful discussions with O. Pokhotelov and comments of both referees are appreciated.

References

- Blagoveschenskaya, N.F., V.M. Vystavnoy, I.A. Shumilov, R.M. Ernandes, and L.P. Sukhares, 1990. Modification of ionosphere caused by launching of the Space Shuttle on September 29, 1988, *Geomagn. Aeronomy*, **30**, N3, 512-514.
- Belyaev, P.P., T. Bosinger, S.V. Isaev, V.Yu. Trakhtengerts, and J. Kangas, 1999. First evidence at high latitudes for the ionospheric Alfvén resonator, *J. Geophys. Res.*, **104**, 4305-4317.

- Borisov, N.D., V.N. Oraevskiy and Yu.A. Ruzin, Generation of MHD fields in the ionosphere by an expanding plasma cloud, *Geomagn. Aeronomy*, 28, N6, 933-939, 1988.
- Bosinger, T., K. Alanko, J. Kangas, H. Opgenoorth, and W. Baumjohann, 1981. Correlation between PiB type magnetic micropulsations, auroras and equivalent current structures during two isolated substorms, *J. Atmosph. Terr.Phys.*, **43**, 933-945.
- Danilushkin, A.I., V.V. Krasnoselskikh, V.V. Mishukin, P.A. Morosov, and A.E. Reznikov, 1988. Variation in the level of ELF noises on the Earth surface in the magnetically conjugated region during the "Waterhole" experiment, *Doklady AN SSSR*, **299**, N1, 84-88.
- Dea J.Y., W. Van Bise, E.A. Rauscher and W.M. Boerner, 1991. Observations of ELF signatures arising from space vehicle disturbances of the ionosphere, *Can. J. Phys.*, **69**, N8-9, 959-965.
- Fujita, S., 1988. Duct propagation of hydromagnetic waves in the upper ionosphere. 2. Dispersion characteristics and loss mechanism, *J. Geophys. Res.*, **93**, No.12, 14674-14682.
- Gorely, K.I., V.K. Lampei, and A.V. Nikolsky, 1994. Ionospheric effects of space vehicles launches, *Geomagn. Aeronomy*, **34**, N3, 158-161.
- Grebnev, I.A., and P.V. Henkin, 1993. Modeling of magnetic and electric fields disturbances under fly-apart of plasma-producing compound in the ionosphere, *Kosmicheskie issledovanija (Space Research)*, **31**, N1, 143-149.
- Greinfinger, C., and P.S. Greinfinger, 1968. Theory of hydromagnetic propagation in the ionospheric wave guide, *J. Geophys. Res.*, **73**, 7473-7490.
- Zamyshlyayev, B.V., S.N. Prijatkin, and E.L. Stupitsky, 1993. Early stage of the fly-apart of partially ionized barium in geomagnetic field, *Kosmicheskie issledovanija (Space Research)*, **31**, N2, 55-62.
- Karlov, V.D., S.I. Kozlov, and V.P. Kudrjavitzev, 1980. Large-scale disturbances in the ionosphere arising during the flight of rocket with running engine (a review), *Kosmicheskie issledovanija (Space Research)*, **18**, N2, 266-277.
- Kelley, M.C., U.V. Fahleson, G. Holmgren, R. Bostrom, P.M. Kintner, and E. Kudeki, 1980. Generation and propagation of an electromagnetic pulse in the Trigger experiment and its possible role in electron acceleration, *J. Geophys. Res.*, **85**, N10, 5055-5060.
- Koons, H.C., and M.B. Pongratz, 1979. Ion cyclotron waves generated by an ionospheric barium injection, *J. Geophys. Res.*, **84**, N2, 533-536.
- Kozlov S.I., and N.V. Smirnova, 1992. Creation's methods and means of the artificial formations in space and characteristics of the disturbances. 1., *Kosmicheskie issledovanija (Space Research)*, **30**, N4, 495-523.
- Mendillo, M., 1975. A sudden vanishing of the ionospheric F-region due to the launch of Skylab, *J. Geophys. Res.*, **80**, N16, 2217-2228.
- Mendillo, M., 1988. Ionospheric holes: a review of theory and recent experiments, *Adv. Space Res.*, **8**, N1, 51-62.

- Pokhotelov, O.A., M. Parrot, V.A. Pilipenko, E.N. Fedorov, V.V. Surkov, and V.A. Gladyshev, 1995. Response of the ionosphere to natural and man-made acoustic sources, *Ann. Geophysicae*, **13**, 10197-10210.
- Smirnova N.V., Kozlov S.I., and Kozik E.A., 1995. Influence of solid fuel rockets on the Earth's ionosphere. 2. E and E-F regions, *Kosmicheskie issledovanija (Space Research)*, **33**, N2, 115.
- Tagirov, V.R., V.A. Arinin, U. Brandstrom, A. Pajunpaa, and V.V. Klimenko, 2000. Atmospheric optical phenomena caused by powerful rocket launches, *J. Spacecraft and Rockets*, **37**, N6, 812-821.
- Vetchinkin, N.V., L.V. Granitsky, Yu.V. Platov, and A.I. Sheikhet, 1993. Optical phenomena in near-Earth medium caused by operation of rocket and satellite boosters. I. Ground and satellite observations of artificial during rocket launches, *Kosmicheskie issledovanija (Space Research)*, **31**, N1, 93-100.
- Yau, A.W., B.A. Whalen, M.B. Pongratz, and G. Smith, 1981. Observations of particle participation, electric field and optical morphology of an artificially perturbed auroral arc: project "Waterhole", *J. Geophys. Res.*, **86**, NA7, 5601-5613.
- Yau, A.W., and B.A. Whalen, 1988. Auroral perturbation experiments, *Adv. Space Res.*, **8**, N1, 67-77.